given

$$C/ScY_i'+fY_i=-\dot{m}_i/\sqrt{2\rho_e\mu_e\alpha} \quad (10d)$$

at the wall. Here $\dot{m}_i$ is the vaporization rate of species i ($\dot{m}_i=0$ except for i=C, C_2, and C_3), which is given by the Knudsen-Langmuir equation

$$\dot{m}_i=\alpha_i\sqrt{M_i/2\pi RT_w}\,(p_{v,i}-Y_ip_e\bar{M}/M_i)_w \ \text{g/cm}^2\text{-s} \quad (11)$$

where α_i is the vaporization coefficient of the species i, p_e is the total pressure, and $p_{v,i}$ is the vapor pressure of the ith species at the wall temperature, which is obtained from thermodynamics.

Results and Discussion

The equations and the boundary conditions just described are complete and ready for numerical calculation. As an exact solution is required, no approximation is introduced in the solution method. The initial value of $f(0)$, $f''(0)$, $\theta'(0)$, and $Y_i(0)$ should be determined. This determination is made such that, as $Y_i(0)$ is changed, $f(0)$ changes according to Eqs. (11) and (10a). Thus $f''(0)$ must be chosen very carefully. The well-known Newton-Raphson method failed to find these values, and the relaxation method was adopted instead for a small vaporization rate. Many trials were required to obtain a solution. In the calculation, hydrogen and methylidyne were assumed to be dissociated, since their equilibrium concentrations at this high temperature of interest (T_e = 12,000 K and T_w = 3000 K) are much smaller than the other species. The composition of the external stream is taken from the Jupiter nominal atmosphere.

The results are shown in Fig. 1 and Table 1. Significant differences were not found in the temperature and velocity profiles in the boundary layer between frozen and nonequilibrium chemistry because of the small vaporization rate (T_w = 3000 K). But profiles of carbon species for nonequilibrium flow are significantly different from those for frozen flow (Fig. 1). This shows the excess of diatomic carbon (a very important species for heat shielding in Jupiter entry) in the gas-phase boundary layer if it is calculated from the frozen boundary-layer equation. If the surface condition is taken as equilibrium, the difference between frozen and equilibrium flow is not significant, because $Y_i(0)$ is the same for each case (see Fig. 11 in Ref. 1).

Table 1 shows that the vaporization rate of monatomic carbon is negative; in other words, monatomic carbon is adsorbed on the wall because of high dissociation rates of di- and triatomic carbon in the gas-phase boundary layer. This conclusion does not result from frozen boundary-layer equations or from equilibrium surface conditions. Table 1 also shows that the vaporization rates of di- and triatomic carbon for a nonequilibrium flow case are much larger than those for the frozen flow case. From Fig. 1 and Table 1, it is concluded that 1) the surface condition should be nonequilibrium, and 2) in the gas-phase boundary layer, the compositions are far from those of frozen flow at the high temperature of interest.

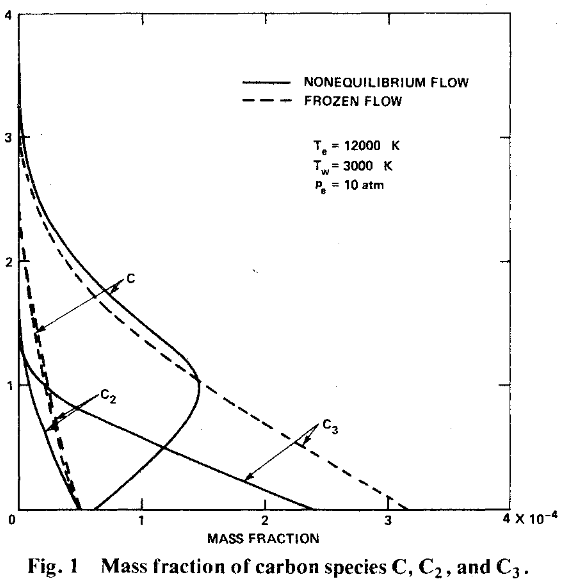

Fig. 1 Mass fraction of carbon species C, C_2, and C_3.

Table 1 Dimensionless vaporization rates[a]

Chemical behavior in boundary layer	Dimensionless vaporization rate, $\times 10^{-4}$		
	$\dot{m}_C$	$\dot{m}_{C2}$	$\dot{m}_{C3}$
Frozen	0.27	0.29	1.90
Nonequilibrium	−1.23	0.45	2.79

[a] $\dot{m}_i=\dot{m}_i/\sqrt{2\rho_e\mu_e\alpha}$.

Acknowledgments

Helpful discussions with S. Tsugé of Nielsen Engineering and Research, Inc., and J. T. Howe of NASA Ames Research Center are gratefully acknowledged.

References

[1] Liu, T.-M. and Davy, W. D., "Nonequilibrium Boundary Layer at a Stagnation Point for a Hydrogen-Helium Stream Over Ablating Graphite," *Acta Astronautica*, Vol. 1, March-April 1974, pp. 485-503.

[2] Fay, J. A. and Riddell, F. R., "Theory of Stagnation Point Heat Transfer in Dissociated Air," *Journal of the Aeronautical Sciences*, Vol. 25, Feb. 1958, pp. 73-85.

[3] Takano, A. and Suzuki, T., "Nonequilibrium Boundary Layer of a Dissociated Gas Over a Catalytic Flat Plate," *Transactions of the Japan Society of Aero Space Sciences*, Vol. 11, No. 19, 1968, pp. 44-59.

[4] Brokaw, R. S., "Viscosity of Gas Mixtures," NASA TN D-4496, April 1968.

[5] Gray, P. and Wright, P. G., "A Comparison of Experimental and Theoretical Values of Thermal Conductivity of Binary Mixtures of Nitrogen and Hydrogen," *Proceedings of Royal Society (London)*, Vol. A267, May 1962, pp. 408-416.

[6] Hirschfelder, J. O., Curtiss, C. F., and Bird, R. B., *Molecular Theory of Gases and Liquids*, Wiley, New York, 1954, p. 14.

[7] Svehla, R. A., "Estimated Viscosities and Thermal Conductivities of Gases at High Temperature," NASA TR R-132, 1962.

[8] Hansen, C. F., "Estimation of the Collision-induced Dissociation Rates of Diatomic and Triatomic Molecules," General Motors Defense Research Lab., TR 64-14, Feb. 1964.

A New Method of Nozzle Design

Ryuji Ishii*
Kyoto University, Kyoto, Japan

I. Introduction

IN the aerodynamic design of a convergent-divergent supersonic nozzle, the nozzle must be treated in three parts—the subsonic section, the throat, and the supersonic section. The analysis of the flowfield in the throat portion of the nozzle is, in most cases, the key to the design problem,

Received Jan. 12, 1978; revision received March 28, 1978.

Index categories: Nozzle and Channel Flow; Subsonic Flow; Transonic Flow.
*Research Assistant, Dept. of Aeronautics. Member AIAA.

because the location of the sonic line and the flow conditions on it are required in order to initiate the supersonic design.[1,2] In general, however, it is very difficult (or quite often almost impossible in practice) to construct an exact analytical solution to the problem. Therefore, many efforts have already been devoted to solving the transonic flow near the geometric throat.[3-5]

In order to avoid such a difficulty in relation to the transonic problem, in this paper the design problem of the axially symmetric supersonic nozzle is treated by an inverse method. In this approach the nozzle contour is determined for prescribed flow conditions on a reference streamline, which may be the nozzle axis or another nozzle wall.

The analysis technique employed here is similar to the streamline methods developed by Oswatitsch,[6] and Uchida and Yasuhara.[7] Our scheme differs from the previous ones in the abandonment of the usual stream function as an independent or dependent variable in the system of basic equations. This is important because the introduction of the stream function leads to the necessity of iteratively solving for the streamline pattern and this usually greatly complicates the analysis.

II. Basic Equations

It is convenient for the present purpose to use the general description of the streamline and the orthogonal trajectory to the streamlines,[6,7]

$$\alpha(\bar{x},\bar{y}) = \text{const along } \frac{d\bar{y}}{d\bar{x}} = -\cot\theta \tag{1}$$

$$\beta(\bar{x},\bar{y}) = \text{const along } \frac{d\bar{y}}{d\bar{x}} = \tan\theta \tag{2}$$

where $\bar{x}$ is the distance along the nozzle axis measured from the throat, $\bar{y}$ is the distance from the axis, and θ is the flow angle relative to the $\bar{x}$ axis. Here, the flow equations are written with (α,β) as the independent variables.

Now, the dimensionless quantities are introduced by

$$x=\bar{x}/\bar{L},\quad y=\bar{y}/\bar{L},\quad \rho=\bar{\rho}/\bar{\rho}_*,\quad V=\bar{V}/\bar{a}_*,\quad p=\bar{p}/\bar{p}_* \tag{3}$$

where $\bar{L}$ is a reference nozzle length, and $\bar{\rho}$, $\bar{V}$, $\bar{p}$, and $\bar{a}$ are the density, velocity, pressure, and speed of sound of the gas, respectively, of which the last is defined by

$$\bar{a}^2 = \gamma(\bar{p}/\bar{\rho}) \tag{4}$$

where γ is the ratio of the specific heats. The asterisk denotes the critical (sonic) conditions and the quantities $\bar{\rho}_*$, $\bar{p}_*$, and then $\bar{a}_*$ may not be constants but functions of β. These sonic conditions $\bar{\rho}_*$ and $\bar{p}_*$ are obtained uniquely from the reservoir conditions which are not always required to be uniform across the streamline and are, therefore, assumed known.

Using the dimensionless quantities introduced previously, we can describe the system of basic equations for an inviscid, nonconducting flow as:

$$\frac{1}{\rho V}\frac{\partial}{\partial\alpha}(\rho V) - \frac{(\partial y/\partial\alpha)}{(\partial x/\partial\beta)}\frac{\partial\theta}{\partial\beta} + \frac{1}{y}\frac{\partial y}{\partial\alpha} = 0 \tag{5}$$

$$\rho V^2\frac{\partial\theta}{\partial\alpha} - \frac{1}{\gamma}\frac{(\partial y/\partial\alpha)}{(\partial x/\partial\beta)}\frac{\partial p}{\partial\beta} = \frac{1}{\gamma}\frac{(\partial y/\partial\alpha)}{(\partial x/\partial\beta)} p \frac{d}{d\beta}(\ln\bar{p}_*) \tag{6}$$

$$p=\rho^\gamma \tag{7}$$

$$\frac{p}{\rho} = \frac{\gamma+1}{2}\left(1-\frac{\gamma-1}{\gamma+1}V^2\right) \tag{8}$$

$$\frac{\partial y}{\partial\alpha} = \tan\theta\frac{\partial x}{\partial\alpha} \tag{9}$$

$$\frac{\partial y}{\partial\beta} = -\cot\theta\frac{\partial x}{\partial\beta} \tag{10}$$

where Eqs. (9) and (10) are obtained from Eqs. (2) and (1), respectively. It is easy to see that the new independent variables (α,β), which are introduced in Eqs. (9) and (10), are dimensionless.

With Eqs. (9) and (10), Eqs. (5) and (6) can be rewritten, respectively, as

$$\frac{\partial}{\partial\alpha}\ln(\rho V y) + \frac{\partial}{\partial\alpha}\ln\left[\frac{(\partial y/\partial\beta)}{\cos\theta}\right] = 0 \tag{11}$$

$$\frac{\partial}{\partial\beta}\ln\left[\frac{(\partial x/\partial\alpha)}{\cos\theta}\right] - \frac{1}{\gamma}\frac{1}{\rho V^2}\frac{\partial p}{\partial\beta} = \frac{1}{\gamma}\frac{p}{\rho V^2}\frac{d}{d\beta}\ln\bar{p}_* \tag{12}$$

These can be integrated along $\beta=\text{const}$ and $\alpha=\text{const}$, respectively, with the aid of Eqs. (7) and (8) to yield

$$V\left(1-\frac{\gamma-1}{\gamma+1}V^2\right)^{1/(\gamma-1)}\frac{y(\partial y/\partial\beta)}{\cos\theta} = F(\beta) \tag{13}$$

$$\frac{V(\partial x/\partial\alpha)}{\cos\theta}\exp\left[-\int_0^\beta \frac{\gamma+1}{2\gamma}\left(\frac{1}{V^2}-\frac{\gamma-1}{\gamma+1}\right)\frac{d}{d\beta}\ln\bar{p}_* d\beta\right] = G(\alpha) \tag{14}$$

where $\beta=0$ is chosen as the reference streamline (the nozzle axis), and $F(\beta)$ and $G(\alpha)$ are functions of β and α, respectively. Equations (9, 10, 13, and 14) constitute a system of partial differential equations for x, y, V, and θ with respect to α and β.

The boundary conditions which must be satisfied by the system are

$$x=\alpha,\quad y=0,\quad V=\nu(\alpha),\quad \theta=0 \quad \text{at } \beta=0 \tag{15}$$

$$y=\beta \quad \text{at } \alpha=0 \tag{16}$$

where $\nu(\alpha)$ is the prescribed velocity distribution on the reference streamline $\beta=0$ (the nozzle axis). Substituting the boundary conditions, Eqs. (15) and (16), into Eqs. (13) and (14) yields, respectively,

$$F(\beta) = \frac{\beta V(0,\beta)}{\cos\theta(0,\beta)}\left[1-\frac{\gamma-1}{\gamma+1}V(0,\beta)^2\right]^{1/(\gamma-1)} \tag{17}$$

$$G(\alpha) = \nu(\alpha) \tag{18}$$

III. Solution by a Streamtube Method

It is sufficient for our purpose to consider the solution of the system in a domain

$$0\le\beta\le\beta_w \tag{19}$$

where β_w is a constant and represents a streamline along the nozzle wall. This constant β_w is determined so as to satisfy a condition

$$y(\alpha,\beta_w)_{\text{throat}} = y(\alpha,\beta_w)_{\min} = 1 \tag{20}$$

if the half-height at the throat $\bar{r}$ is taken as the reference nozzle length $\bar{L}$. The flow domain, Eq. (19), in the $\alpha\beta$ plane corresponds to a domain $0\le y\le f(x)$ in the xy plane, where $f(x)$ is the nozzle contour to be determined.

The flow domain in the $\alpha\beta$ plane is first divided into a large number of strips by drawing lines on

$$\beta=\beta_i=\begin{cases} 0 & \text{for } i=0 \\ \sum_{j=1}^{i}\Delta\beta_j & \text{for } i\geq 1 \end{cases} \tag{21}$$

where i is a nonnegative integer and $\Delta\beta_j$ ($j=1,2,\ldots, i$) are positive constants which can be specified arbitrarily under a condition of

$$\sum_{j=1}^{n}\Delta\beta_j=\beta_w \tag{22}$$

where n is a positive integer describing the number of strips. It is easy to see that the lines $\beta=\beta_i$ for $i=0$ and $i=n$ represent the nozzle axis and the streamline along the nozzle wall, respectively.

Next, suppose that we can approximate the flow variables in the system by functions of α only in a domain $\beta_i\leq\beta\leq\beta_{i+1}$,

$$P(\alpha,\beta)=P_i(\alpha)=P(\alpha,\beta_i) \tag{23}$$

where P may denote any one of the dependent variables V and θ.

With the boundary conditons of Eqs. (15) and (16), Eq. (13) yields, in conjunction with Eq. (17),

$$\left(\frac{\partial y}{\partial\beta}\right)=\frac{\beta_i}{y(\alpha,\beta_i)}\frac{\cos\theta(\alpha,\beta_i)}{\cos\theta(0,\beta_i)}$$

$$\times\frac{V(0,\beta_i)\left[1-\frac{\gamma-1}{\gamma+1}V(0,\beta_i)^2\right]^{1/(\gamma-1)}}{V(\alpha,\beta_i)\left[1-\frac{\gamma-1}{\gamma+1}V(\alpha,\beta_i)^2\right]^{1/(\gamma-1)}};\quad i\geq 1$$

$$=\left\{\frac{\nu(0)\left[1-\frac{\gamma-1}{\gamma+1}\nu(0)^2\right]^{1/(\gamma-1)}}{\nu(\alpha)\left[1-\frac{\gamma-1}{\gamma+1}\nu(\alpha)^2\right]^{1/(\gamma-1)}}\right\}^{1/2};\quad i=0 \tag{24}$$

at $\beta=\beta_i$. Using Eq. (24), we can get approximately the value of the y coordinate of a streamline for $\beta=\beta_{i+1}$ by

$$y_{i+1}=y(\alpha,\beta_i)+(\partial y/\partial\beta)_{\beta=\beta_i}\Delta\beta_{i+1} \tag{25}$$

Similarly, the x coordinate $x(\alpha,\beta_{i+1})$ is obtained approximated by

$$x_{i+1}=x(\alpha,\beta_i)+(\partial x/\partial\beta)_{\beta=\beta_i}\Delta\beta_{i+1} \tag{26}$$

Combining Eqs. (25) and (26) with the aid of Eqs. (24) and (10) determines the streamline for $\beta=\beta_{i+1}$ in the physical plane.

The flow angle θ on the streamline $\beta=\beta_{i+1}$ can easily be obtained from Eq. (9) in conjunction with Eq. (10) as

$$\theta_{i+1}=\tan^{-1}\left[\frac{(\partial y/\partial\alpha)}{(\partial x/\partial\alpha)}\right]_{\beta=\beta_{i+1}}$$

$$=\tan^{-1}\left\{\frac{\sum_{j=1}^{i+1}\left[\frac{d}{d\alpha}\left(\frac{\partial y}{\partial\beta}\right)_{\beta=\beta_{j-1}}\Delta\beta_j\right]}{1+\sum_{j=1}^{i+1}\left[\frac{d}{d\alpha}\left(\frac{\partial x}{\partial\beta}\right)_{\beta=\beta_{j-1}}\Delta\beta_j\right]}\right\} \tag{27}$$

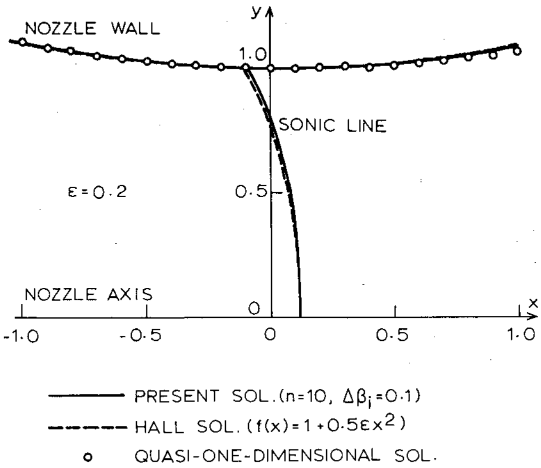

Fig. 1 Nozzle shape and the sonic line for $\epsilon=0.2$.

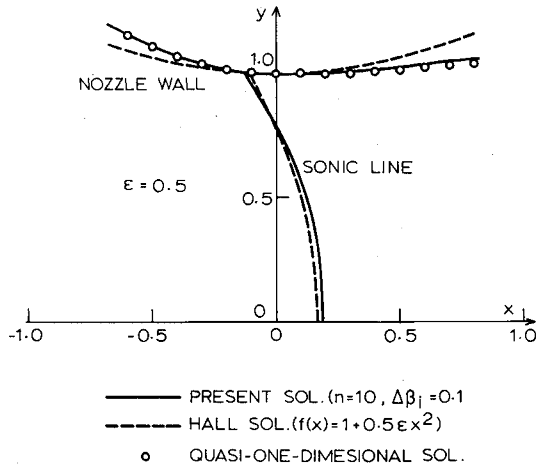

Fig. 2 Nozzle shape and the sonic line for $\epsilon=0.5$.

where use was made of Eqs. (25) and (26). The flow velocity on the streamline $\beta=\beta_{i+1}$ is obtained from Eq. (14) with the aid of Eq. (18) under the assumption of Eq. (23) as

$$V_{i+1}=\frac{\nu(\alpha)\cos\theta_{i+1}}{\left\{1-\sum_{j=1}^{i+1}\frac{d}{d\alpha}\left[\tan\theta_{j-1}\left(\frac{\partial y}{\partial\beta}\right)_{\beta=\beta_{j-1}}\Delta\beta_j\right]\right\}}$$

$$\times\exp\left\{\frac{\gamma+1}{2\gamma}\sum_{j=1}^{i+1}\left[\left(\frac{1}{V_{j-1}^2}-\frac{\gamma-1}{\gamma+1}\right)\ln\left(\frac{p_*(\beta_j)}{p_*(\beta_{j-1})}\right)\right]\right\} \tag{28}$$

Once the streamline (x_{i+1}, y_{i+1}) in the physical plane for $\beta=\beta_{i+1}$ and the flow quantities (θ_{i+1}, V_{i+1}) on it are determined, the streamline (x_{i+2}, y_{i+2}) for $\beta=\beta_{i+2}$ and the flow quantities (θ_{i+2}, V_{i+2}) on it can easily be determined in the same manner. By repeated applications of this procedure, the streamline (x_i, y_i) for any value of i and the flow conditions (θ_i, V_i) on it may be uniquely determined. Especially, the streamline for $i=n$

$$x=x_n=x(\alpha,\beta_w) \tag{29a}$$

$$y=y_n=y(\alpha,\beta_w) \tag{29b}$$

yields the nozzle contour with α as a dummy variable, which is to be finally determined. Equations (29) may, therefore, be taken as the implicit expression of the nozzle contour $y=f(x)$.

IV. Numerical Discussions

In order to evaluate the method developed here and to check its validity and accuracy, the sample calculations have been carried out for the flows of a gas with $\gamma = 1.4$. It is assumed that $\bar{p}_*(\beta) = \text{const}$ and the number of strips n is chosen as 10. Two types of the velocity distribution along the nozzle axis are considered:

$$\nu(\alpha) = 0.96079 + 0.35772\alpha + 0.00556\alpha^2 \quad \text{for } \epsilon = 0.2 \tag{30}$$

$$\nu(\alpha) = 0.94184 + 0.44378\alpha + 0.01389\alpha^2 \quad \text{for } \epsilon = 0.5 \tag{31}$$

where

$$\epsilon = \bar{r}/\bar{R} \tag{32}$$

and where $\bar{R}$ is the radius of curvature of the nozzle contour at the throat. The velocity distributions (30) and (31) are both the solutions in the second approximation of Hall's perturbation method for the nozzle contour

$$f(x) = 1 + \frac{\epsilon}{2} x^2 \tag{33}$$

The numerical results of the nozzle contour and the sonic line for the axial velocity distributions, Eqs. (30) and (31), are shown in Figs. 1 and 2 by the solid lines that are compared with the results obtained by the quasi-one-dimensional approximation and by the inverse application of Hall's method.

For the small value of $\epsilon (= 0.2)$, for which Hall's method is believed to be well applicable and accurate, the present result of the nozzle shape is in good agreement with that of his result, Eq. (33). In the subsonic portion of the throat $(x<0)$, the nozzle shape of the quasi-one-dimensional approximation also agrees well with the two others. It gives, however, a slightly lower value than the others in the supersonic region $(x>0)$. A small difference in the location of the sonic line is found between the present and Hall's results.

For the larger value of $\epsilon (= 0.5)$, for which the validity of Hall's method is in doubt, the nozzle shape of the present method deviates appreciably from his result, but is relatively in good agreement with the quasi-one-dimensional result.

Finally, it must be noted that in order to adequately check the validity of our scheme, it would be necessary to carry out the calculations for larger values of $n (>10)$ and to investigate the convergency of the results with n. These calculations are now being systematically carried out on the electronic digital computer FACOM 230 at the computing center of Kyoto University. The results will be reported in the near future.

References

[1] Hall, I. M., "Transonic Flow in Two-Dimensional and Axially-Symmetric Nozzles," *Quarterly Journal of Mechanics and Applied Mathematics*, Vol. XV, Nov. 1962, pp. 487-508.

[2] Sauer, R., "General Characteristics of the Flow Through Nozzles at Near Critical Speed," NACA TM 1147, June 1947.

[3] Hopkins, D. F. and Hill, D. E., "Effect of Small Radius of Curvature on Transonic Flow in Axisymmetric Nozzles," *AIAA Journal*, Vol. 4, Aug. 1966, pp. 1337-1343.

[4] Kliegel, J. R. and Quan, V., "Convergent-Divergent Nozzle Flows," *AIAA Journal*, Vol. 6, Sept. 1968, pp. 1728-1734.

[5] Kliegel, J. R. and Levine, J. N., "Transonic Flow in Small Throat Radius of Curvature Nozzles," *AIAA Journal*, Vol. 7, July 1969, pp. 1375-1378.

[6] Oswatitsch, K., *Gas Dynamics*, Academic Press, New York, 1956, pp. 254-255.

[7] Uchida, S. and Yasuhara, M., "Rotational Flow Field Behind a Curved Shock Wave Calculated by the Method of Flux Analysis," *Journal of the Aeronautical Sciences*, Vol. 23, Sept. 1956, pp. 830-845.

A Critique of a Second-Order Upwind Scheme for Viscous Flow Problems

Murli M. Gupta* and Ram P. Manohar†
University of Saskatchewan, Saskatoon, Canada

In a recent paper, Atias et al.[1] compared the efficiency of various Navier-Stokes solvers. In particular, they studied a second-order upwind scheme (USO) for discretizing the convective terms in the vorticity transport equation. This Note presents convergence and stability properties of the second-order upwind scheme when applied to a linearized one-dimensional form of the vorticity transport equation. Comparisons are carried out with the existing central difference scheme (CC) and the first-order upwind difference scheme (UFO), and it is found that the second-order upwind scheme is no better than the upwind difference scheme of first order for large Reynolds numbers. Even when the accuracy of the USO is comparable to the accuracy of CC, it is computationally more complex.

Accuracy

The vorticity transport equation for a two-dimensional flow has the form

$$\frac{\partial^2 \omega}{\partial x^2} + \frac{\partial^2 \omega}{\partial y^2} + R\left(\frac{\partial \psi}{\partial x} \cdot \frac{\partial \omega}{\partial y} - \frac{\partial \omega}{\partial x} \cdot \frac{\partial \psi}{\partial y}\right) = 0 \tag{1}$$

In order to solve Eq. (1) numerically, the second derivatives of ω and first derivatives of ψ are replaced by central difference formulas. If the terms $\partial\omega/\partial x$ and $\partial\omega/\partial y$ also are replaced by central differences, the resulting scheme is called the central difference scheme (CC). It is well known that, for large values of the Reynolds number R, the central difference scheme does not yield an accurate solution. An alternative approach is to replace $\partial\omega/\partial x$ and $\partial\omega/\partial y$ by first-order forward or backward differences, depending upon the sign of the velocities $\partial\psi/\partial x$, $\partial\psi/\partial y$. Such a difference is called an upwind difference scheme of first order (UFO). This upwind scheme is known to produce satisfactory solutions for all values of R. The second-order upwind scheme (USO) studied by Atias et al.[1] uses one-sided finite differences of second order to discretize $\partial\omega/\partial x$, $\partial\omega/\partial y$. Such a scheme was studied first by Price et al.[2]

A one-dimensional analog of the vorticity transport equation, Eq. (1), is given by

$$\frac{\partial^2 \omega}{\partial x^2} + \lambda \frac{\partial \omega}{\partial x} = 0, \quad a < x < b \tag{2}$$

with $\omega(a) = \omega_a$, $\omega(b) = \omega_b$. Without loss of generality, we take $a = 0$, $b = 1$, $\omega_a = 0$, and $\omega_b = 1$. The exact solution of Eq. (2) is

$$\omega(x) = (1 - e^{-\lambda x})/(1 - e^{-\lambda}) \tag{3}$$

The upwind difference scheme of second order (USO) for Eq. (2) is given by

$$h^{-2}[u_{i-1} - 2u_i + u_{i+1}] + \lambda(2h)^{-1} \times \begin{Bmatrix} [-3u_i + 4u_{i+1} - u_{i+2}] \\ [3u_i - 4u_{i-1} + u_{i-2}] \end{Bmatrix} = 0 \quad \begin{matrix} \lambda > 0 \\ \lambda < 0 \end{matrix} \tag{4}$$

Received Dec. 9, 1977; revision received March 14, 1978.

Index categories: Computational Methods; Viscous Nonboundary-Layer Flows.

*Visiting Post Doctoral Fellow, Dept. of Mathematics.
†Professor, Dept. of Mathematics.